

Tianyi Shen, Guocan Wang, Peter van der Beek, Matthias Bernet, Yue Chen, Pan Zhang, An Wang, and Kai Cao, 2022, Impacts of late Miocene normal faulting on Yarlung Tsangpo River evolution, southeastern Tibet: GSA Bulletin, <https://doi.org/10.1130/B36210.1>.

## Supplemental Material

### Supplemental Text. Methods

**Figure S1.** Zircon U-Pb concordia diagrams (up) and weighted mean diagrams using the routines in Isoplot (Ludwig, 2012).

**Table S1.** GPS data for all the samples

**Table S2.** Zircon U-Pb analyses of sample 14T24.

**Table S3.** Apatite fission-track data from the Woka Rift flank (U-content analyzed using the laser-ablation method).

**Table S4.** Apatite (U-Th)/He data from the Woka Rift flank.

**Table S5.** Apatite and zircon fission-track data from the Jiacha Gorge (U-content determined using external-detector method).

**Table S6.** Apatite (U-Th)/He data from the Jiacha Gorge.

**Table S7.** Zircon (U-Th)/He data from the Jiacha Gorge.

## METHODS

### Zircon U-Pb Dating

Sample 14T24 was zircon U-Pb dated using laser ablation multi-collector inductively coupled plasma mass spectrometry (LA-MC-ICPMS) at the State Key Laboratory of Geological Processes and Mineral Resources (GPMR), China University of Geosciences (Wuhan). We used a spot diameter of 32  $\mu\text{m}$ ; data reduction procedures are described in Liu et al. (2008). Zircon 91500 was used as the external standard for U-Pb dating, and was analyzed twice for every six analyses. Time-dependent drifts of U-Th-Pb isotopic ratios were corrected using linear interpolation according to the variations of the external standard. To monitor age reproducibility and instrument stability, four GJ-1 zircon standards were inserted at the beginning and end of each run, making sure the results are consistent with recommended values ( $608.5 \pm 0.4$  Ma; Jackson et al., (2004)). Each analysis incorporated a background acquisition of  $\sim 20$ – $30$  s (gas blank) followed by 50 s of data acquisition from the sample. The Agilent Chemstation was used for the acquisition of individual analyses. Off-line selection and integration of background and analyzed signals, time-drift correction and quantitative calibration for trace-element analyses and U-Pb dating were performed by ICPMSDataCal (Liu et al., 2008). Analysis data are presented in Table S1, and Pb/U concordia diagrams constructed using the Isoplot routines (Ludwig, 2012) are shown in Fig. S1.

## **Fission-Track Dating**

### ***Laser ablation method***

AFT analysis of samples from the Woka Rift footwall used a laser ablation inductively coupled plasma mass spectrometry method following Tian et al. (2014). Apatites were mounted in epoxy resin on glass slides, ground, and polished to an optical finish to expose internal grain surfaces. Mounts were etched in 5-M HNO<sub>3</sub> for 20 s at 21 °C to reveal fossil tracks. Track counting was carried out under a magnification of 1000 (100 × 10) with a Zeiss microscope, according to the procedure described in Garver (2004), at the GPMR, China University of Geosciences (Wuhan). Uranium measurements of selected grains were carried out on an Agilent 7700 ICP-MS using a pulsed laser with a wavelength of 213 nm. Laser ablation under consistent laser conditions (32-μm diameter beam size and 6-Hz repetition rate) was applied to selected grains and the NIST-612 uranium standard for 25 s. The <sup>238</sup>U/<sup>43</sup>Ca ratio of the NIST-612 glass and apatite <sup>43</sup>Ca were used as internal standards to correct for drift in instrument sensitivity and variations in ablation volume between dated grains, respectively. Quantitative calibration for trace-element analyses was performed with ICPMSDataCal (Liu et al., 2008). Single-grain and pooled AFT ages were calculated according to Hasebe et al. (2004). Central ages were estimated from the single-grain ages and errors according to the formulas given by Galbraith (2005), using the Newton-Raphson method.

### ***External detector method***

The samples from the Jiacha Gorge were ZFT and AFT dated using the external detector method described by Garver (2004). Samples were prepared and analyzed at the Institut des Sciences de la Terre (ISTerre, Grenoble, France). Apatite grains were mounted in epoxy, polished to expose internal crystal surfaces, and etched with 5.5 M HNO<sub>3</sub> for 20 s at 21 °C. Zircons were mounted in Teflon® sheets, polished, and etched at 228 °C in a laboratory oven in a eutectic NaOH - KOH melt. Apatite samples were irradiated together with IRMM 540R glass standards and Durango and Fish Canyon Tuff age standards. Zircon samples were irradiated together with IRMM541 glass standards and Fish Canyon Tuff and Buluk Tuff age standards. After irradiation, the mica sheets covering all samples and standards were etched for 18 min at 21 °C in 48% HF. Fission tracks were counted in at least 20 grains where possible; ages were calculated using the Zeta-calibration method and the standard fission-track age equation (Hurford and Green, 1982). The size of the etch-pit diameter parallel to the c axis (Dpar) was also determined, as it is a kinetic parameter used in thermal history modeling (Ketcham et al., 1999).

## **Apatite (U-Th)/He Dating**

Apatite (U-Th)/He analysis of the samples from Woka Rift were conducted in the Arizona Radiogenic Helium Dating Laboratory, the University of Arizona, using the methods described in Reiners and Nicolescu (2006). Apatites which are clarity, lack of visible inclusions and half-width >60 μm were selected for analysis (Farley et al., 1996). Each sample, four grains were placed in 1 mm Nb foil envelopes and loaded into a vacuum laser cell and heated to ~900°C for several minutes to release their <sup>4</sup>He gas. The released <sup>4</sup>He gas was spiked with a known volume of <sup>3</sup>He and the <sup>4</sup>He/<sup>3</sup>He isotopic ratio was measured with a quadrupole mass spectrometer. Degassed grains were dissolved to determine the molar contents of parent nuclides

(U, Th, and Sm) and analyzed via isotope-dilution using an inductively coupled plasma mass spectrometer (Reiners and Nicolescu, 2006). A corrected date was calculated using an alpha-ejection correction factor from volume dimensions of individual grains (Farley, 2002). Durango Apatite were used as apatite standards with each batch of samples analyzed and served as an additional check on analytical accuracy.

The other samples from the Jiacha Gorge were conducted at the School of Earth Sciences, University of Melbourne, using the method described in Tian et al. (2018). Grains with good-quality euhedral morphologies were loaded into platinum capsules and outgassed under vacuum at ca. 900 °C for 5 min, using a fiber optically coupled diode laser with 820 nm wavelength. <sup>4</sup>He abundances were determined as an isotope ratio using a pure <sup>3</sup>He spike that has been calibrated against an independent <sup>4</sup>He standard. Apatite U-Th-Sm data were obtained using an Agilent 7700 quadrupole ICP-MS after total dissolution of the outgassed apatite aliquots in HNO<sub>3</sub>. Ages were corrected for alpha ejection (FT correction; Farley et al., 1996). Durango apatite was run as standards with each batch of samples analyzed and served as an additional check on analytical accuracy.

### **Zircon (U-Th)/He Dating**

Two zircon (U-Th)/He samples were analyzed at the (U-Th)/He laboratory in the Institute of Geology, China Earthquake Administration. Detailed analysis procedures are presented in the Li et al. (2017). The grains were handpicked according to morphology, clarity, size (~60–120 μm width and ~150–300 μm length) and were inclusion-free as confirmed using an electron microprobe. The length and width of each grain was measured to calculate the ratio between surface and volume, alpha ejection correction factor (*FT*, Farley et al., 1996), and equivalent spherical radius. He diffusion experiments followed the procedures described in detail by Reiners et al. (2002) involving cycled step-heating of the crystals in a high vacuum chamber by a light bulb projected through a sapphire window. Step heating diffusion experiments were performed on single grain zircons, while multigrain aliquots of zircons with approximately radius were analyzed. The samples were subsequently heated a second time to re-extract the He to verify complete outgassing, and <sup>4</sup>He results were corrected using the measured blank. U and Th contents were determined using isotope dilution inductively coupled plasma mass spectrometry. The ages were calculated using the absolute amounts of parent U and Th and daughter He and were then corrected using standard alpha ejection correction procedures (Farley et al., 1996). Replicate analyses of Penglai zircon (Li et al., 2017) as standards during these analyses yielded weight mean ages of  $3.80 \pm 0.11$  Ma ( $2\sigma$ ,  $n = 2$ ) which could guarantee the analytical accuracy.

### **REFERENCES CITED**

- Brandon, M.T., 1992, Decomposition of fission-track grain-age distributions: American Journal of Science, v. 292, p. 535–564, <https://doi.org/10.2475/ajs.292.8.535>.
- Farley, K.A., Wolf, R.A., and Silver, L.T., 1996, The effects of long alpha-stopping distances on (U-Th)/He ages: Geochimica et Cosmochimica Acta, v. 60, p. 4223–4229, [https://doi.org/10.1016/S0016-7037\(96\)00193-7](https://doi.org/10.1016/S0016-7037(96)00193-7).
- Farley, K.A., 2002, (U-Th)/He dating: Techniques, calibrations, and applications: Reviews in Mineralogy and Geochemistry, v. 47, p. 819–844, <https://doi.org/10.2138/rmg.2002.47.18>.

- Galbraith, R.F., 2005, Statistics for fission track analysis: Chapman and Hall/CRC, <https://doi.org/10.1201/9781420034929>.
- Garver, J.I., 2004, Fission-track Laboratory Procedures at Union College, 3, 2.95.
- Hasebe, N., Barbarand, J., Jarvis, K., Carter, A., and Hurford, A.J., 2004, Apatite fission-track chronometry using laser ablation ICP-MS: *Chemical Geology*, v. 207, p. 135–145, <https://doi.org/10.1016/j.chemgeo.2004.01.007>.
- Hurford, A.J., and Green, P.F., 1982, A users guide to fission-track dating calibration: *Earth and Planetary Science Letters*, v. 59, p. 343–354, [https://doi.org/10.1016/0012-821X\(82\)90136-4](https://doi.org/10.1016/0012-821X(82)90136-4).
- Jackson, S.E., Pearson, N.J., Griffin, W.L., and Belousova, E.A., 2004, The application of laser ablation-inductively coupled plasma-mass spectrometry to in situ U-Pb zircon geochronology: *Chemical Geology*, v. 211, p. 47–69, <https://doi.org/10.1016/j.chemgeo.2004.06.017>.
- Ketcham, R.A., Donelick, R.A., and Carlson, W.D., 1999, Variability of apatite fission-track annealing kinetics: III. Extrapolation to geological time scales: *The American Mineralogist*, v. 84, p. 1235–1255, <https://doi.org/10.2138/am-1999-0903>.
- Li, Y., Zheng, D., Wu, Y., Wang, Y., He, H., Pang, J., Wang, Y., and Yu, J., 2017, A Potential (U-Th)/He Zircon Reference Material from Penglai Zircon Megacrysts: *Geostandards and Geoanalytical Research*, v. 41, p. 359–365, <https://doi.org/10.1111/ggr.12168>.
- Liu, Y., Hu, Z., Gao, S., Guenther, D., Xu, J., Gao, C., and Chen, H., 2008, In situ analysis of major and trace elements of anhydrous minerals by LA-ICP-MS without applying an internal standard: *Chemical Geology*, v. 257, p. 34–43, <https://doi.org/10.1016/j.chemgeo.2008.08.004>.
- Ludwig, K., 2012, User's manual for Isoplot 3.75. A geological toolkit for Microsoft Excel: Berkeley Geochronology Center Special Publication No. 5.
- Reiners, P.W., Farley, K.A., and Hickey, H.J., 2002, He diffusion and (U-Th)/He thermochronometry of zircon: Initial results from Fish Canyon Tuff and Gold Butte: *Tectonophysics*, v. 349, p. 297–308, [https://doi.org/10.1016/S0040-1951\(02\)00058-6](https://doi.org/10.1016/S0040-1951(02)00058-6).
- Reiners, P.W., and Nicolescu, S., 2006, Measurement of parent nuclides for (U-Th)/He chronometry by solution sector ICP-MS: ARHDL Report, 1.
- Tian, Y., Kohn, B.P., Gleadow, A.J.W., and Hu, S., 2014, A thermochronological perspective on the morphotectonic evolution of the southeastern Tibetan Plateau: *Journal of Geophysical Research. Solid Earth*, v. 119, p. 676–698, <https://doi.org/10.1002/2013JB010429>.
- Tian, Y., Li, R., Tang, Y., Xu, X., Wang, Y., and Zhang, P., 2018, Thermochronological constraints on the late Cenozoic morphotectonic evolution of the Min Shan, the eastern margin of the Tibetan Plateau: *Tectonics*, v. 37, p. 1733–1749, <https://doi.org/10.1029/2017TC004868>.

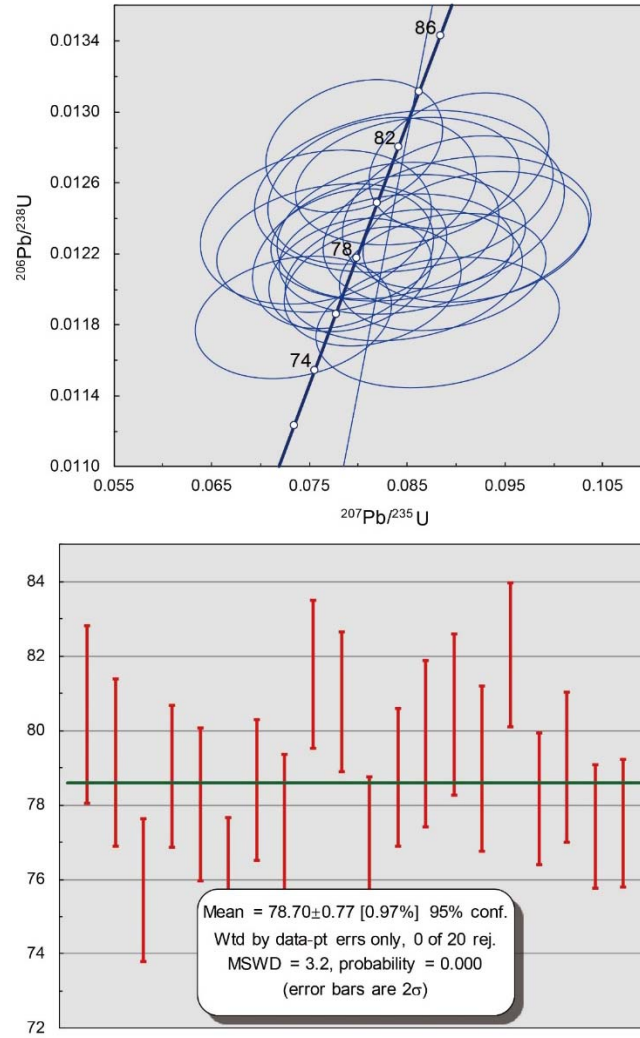


**Figure S1.** Zircon U-Pb concordia diagrams (up) and weighted mean diagrams using the routines in Isoplot (Ludwig, 2012).

TABLE S1 GPS DATA FOR ALL THE SAMPLES

Sample No.	Lon. (°E)	Lat. (°N)	Elevation (m)
17T03	92.36676	29.33777	5265
17T04	92.37554	29.33516	5080
17T05	92.37566	29.35022	4858
17T06	92.37646	29.35143	4797
17T07	92.36983	29.35850	4622
17T08	92.36795	29.3578	4560
14T20	92.41035	29.27395	4191
14T21	92.41183	29.27353	4058
14T22	92.41380	29.27148	3912
14T24	92.41312	29.26393	3660
14T18	92.41693	29.26123	3477
14T26	92.39937	29.25495	3376

TABLE S2. ZIRCON U-PB ANALYSES OF SAMPLE 14T24.

	Pb	Th	U	207Pb/206Pb		207Pb/235U		206Pb/238U			207Pb/206Pb		207Pb/235U		206Pb/238U		
	Total	232	238	Ratio	1sigma	Ratio	1sigma	Ratio	1sigma	rho	Age (Ma)	1sigma	Age (Ma)	1sigma	Age (Ma)	1sigma	Concordance
	ppm	ppm	ppm														
14T24-01	35.8	368	1221	0.0490	0.0038	0.0847	0.0063	0.0126	0.0002	0.2019	150.09	170.35	82.52	5.86	80.42	1.19	97%
14T24-02	45.0	547	1627	0.0444	0.0028	0.0757	0.0048	0.0124	0.0002	0.2248	error		74.06	4.55	79.14	1.13	93%
14T24-03	59.4	692	1837	0.0548	0.0033	0.0881	0.0051	0.0118	0.0002	0.2211	405.61	169.43	85.77	4.75	75.70	0.96	87%
14T24-04	92	1135	2322	0.0549	0.0031	0.0920	0.0047	0.0123	0.0002	0.2379	409.31	124.06	89.40	4.40	78.77	0.96	87%
14T24-05	80	998	2243	0.0473	0.0024	0.0785	0.0038	0.0122	0.0002	0.2735	64.91	124.06	76.70	3.57	78.02	1.02	98%
14T24-06	74	854	2330	0.0450	0.0026	0.0734	0.0041	0.0118	0.0001	0.2120	error		71.88	3.89	75.88	0.90	94%
14T24-07	73	897	2006	0.0461	0.0029	0.0773	0.0048	0.0122	0.0001	0.1945	400.05	-253.67	75.61	4.53	78.40	0.94	96%
14T24-08	66.0	800	1911	0.0504	0.0029	0.0846	0.0050	0.0121	0.0002	0.2136	213.04	133.32	82.50	4.64	77.42	0.96	93%
14T24-09	120	1466	2881	0.0517	0.0023	0.0903	0.0037	0.0127	0.0002	0.2963	272.29	99.99	87.80	3.49	81.52	1.00	92%
14T24-10	100	1223	2307	0.0497	0.0028	0.0850	0.0047	0.0126	0.0001	0.2118	188.97	135.17	82.86	4.39	80.78	0.94	97%
14T24-11	127	1761	2914	0.0492	0.0023	0.0815	0.0037	0.0120	0.0001	0.2506	166.75	104.62	79.53	3.47	77.02	0.87	96%
14T24-12	69.4	802	1944	0.0499	0.0032	0.0841	0.0053	0.0123	0.0001	0.1873	190.82	156.46	82.01	4.98	78.75	0.93	95%
14T24-13	71	850	1884	0.0530	0.0030	0.0898	0.0046	0.0124	0.0002	0.2730	327.84	127.76	87.28	4.32	79.66	1.12	90%
14T24-14	75	938	1866	0.0468	0.0024	0.0814	0.0044	0.0126	0.0002	0.2526	42.69	118.51	79.46	4.09	80.43	1.08	98%
14T24-15	78	1050	1504	0.0538	0.0034	0.0901	0.0056	0.0123	0.0002	0.2280	364.87	140.73	87.59	5.21	78.97	1.11	89%
14T24-16	123	1497	2997	0.0452	0.0021	0.0796	0.0037	0.0128	0.0002	0.2563	error		77.76	3.48	82.04	0.97	94%
14T24-17	49.7	577	1670	0.0499	0.0030	0.0839	0.0049	0.0122	0.0001	0.1939	190.82	134.24	81.81	4.59	78.17	0.88	95%
14T24-18	92	1202	2270	0.0491	0.0028	0.0831	0.0046	0.0123	0.0002	0.2286	150.09	133.32	81.01	4.36	79.02	1.00	97%
14T24-19	165	2295	3613	0.0473	0.0020	0.0792	0.0034	0.0121	0.0001	0.2498	64.91	96.29	77.38	3.21	77.42	0.83	99%
14T24-20	97	1352	2346	0.0530	0.0026	0.0886	0.0043	0.0121	0.0001	0.2293	327.84	109.25	86.23	4.01	77.52	0.86	89%

Note: Best age is determined from  $^{206}\text{Pb}/^{238}\text{U}$  age for analyses with  $^{206}\text{Pb}/^{238}\text{U}$  age <1000 Ma.

TABLE S3. APATITE FISSION-TRACK DATA FROM THE WOKA RIFT FLANK (U-CONTENT ANALYZED USING THE LASER-ABLATION METHOD).

Sample No.	Elevation (m)	No. of Grains	Spontaneous tracks		Pooled $^{238}\text{U}^*$ (ppm)	Pooled Age $\pm 1\sigma$ (Ma) $^\dagger$	$P(\chi^2)^\S$ (%)	Age Dispersion (%)
			n	Density ( $10^5 \text{ cm}^{-2}$ )				
17T03	5265	20	57	0.915	15.08	<b>11.6 <math>\pm</math> 0.8</b>	42	0
17T04	5080	15	75	2.785	46.27	<b>12.1 <math>\pm</math> 0.8</b>	30	0
17T05	4858	16	91	2.281	37.10	<b>12.6 <math>\pm</math> 0.6</b>	12	0
17T06	4797	22	117	1.089	18.05	<b>11.9 <math>\pm</math> 0.5</b>	21	0
17T08	4560	23	51	0.515	8.36	<b>12.2 <math>\pm</math> 0.8</b>	22	0
DUR $^\#$		46	800	2.151	13.14	<b>32.5 <math>\pm</math> 1.1</b>	62	0

\* Pooled uranium content of all grains measured by LA-ICP-MS.

$^\dagger$  Pooled AFT ages of all grains.

$^\S$  P-value of  $\chi^2$  for (No. of Grains – 1) degrees of freedom.

$^\#$  Durango apatite fission-track dating standards, with reference ages constrained by previous studies (McDowell et al., 2005).



TABLE S4. APATITE (U-TH)/HE DATA FROM THE WOKA RIFT FLANK.

Sample	<sup>4</sup> He (nmol)	Mass (mg)	Mean F <sub>T</sub> <sup>*</sup>	U ppm	Th ppm	Sm ppm	Th/U	[eU] <sup>†</sup> ppm	Uncorrected Age (Ma)	Age (Ma)	Error (±1σ)	Weighted Mean age (Ma)	Error (±1σ)
17T03_Ap1	0.48	0.003290	0.756	13.21	4.49	317.86	0.348	14.27	6.08	<b>8.0</b>	<b>0.1</b>	<b>7.5</b>	<b>0.8</b>
17T03_Ap2	0.18	0.005867	0.815	5.64	1.92	192.31	0.349	6.09	5.34	<b>6.5</b>	<b>0.1</b>		
17T03_Ap3	0.54	0.006712	0.789	15.48	5.72	386.55	0.379	16.83	5.77	<b>7.3</b>	<b>0.1</b>		
17T03_Ap4	0.56	0.004129	0.761	15.53	4.10	325.17	0.271	16.49	6.20	<b>8.1</b>	<b>0.1</b>		
17T05_Ap1	1.56	0.008246	0.792	47.44	6.82	197.83	0.147	49.04	5.88	<b>7.4</b>	<b>0.1</b>	<b>7.7</b>	<b>1.0</b>
17T05_Ap2	0.84	0.002971	0.745	24.31	22.82	186.12	0.963	29.67	5.18	<b>7.0</b>	<b>0.1</b>		
17T05_Ap3 <sup>§</sup>	2.27	0.004642	0.772	42.76	9.67	191.75	0.232	45.03	9.30	<b>12.1</b>	<b>0.2</b>		
17T05_Ap4	2.02	0.003136	0.724	55.95	19.24	218.33	0.353	60.47	6.17	<b>8.6</b>	<b>0.1</b>		
17T06_Ap1	1.91	0.002442	0.720	43.94	7.64	309.79	0.178	45.74	7.70	<b>10.7</b>	<b>0.1</b>	<b>9.9</b>	<b>1.5</b>
17T06_Ap2	1.66	0.003348	0.751	34.47	5.53	304.49	0.165	35.77	8.50	<b>11.3</b>	<b>0.2</b>		
17T06_Ap3	0.31	0.002514	0.728	9.06	0.91	303.85	0.103	9.27	5.90	<b>8.1</b>	<b>0.1</b>		
17T06_Ap4	1.03	0.005054	0.783	24.54	3.81	326.69	0.159	25.43	7.43	<b>9.5</b>	<b>0.1</b>		
17T07_Ap1	1.02	0.002231	0.755	29.17	19.88	76.51	0.699	33.84	5.55	<b>7.4</b>	<b>0.1</b>	<b>7.2</b>	<b>0.7</b>
17T07_Ap2	0.27	0.001611	0.722	10.16	3.00	36.60	0.303	10.86	4.66	<b>6.5</b>	<b>0.2</b>		
17T07_Ap3	0.41	0.001966	0.731	13.20	9.21	77.45	0.716	15.36	4.91	<b>6.8</b>	<b>0.1</b>		
17T07_Ap4	0.50	0.006372	0.792	12.18	10.68	58.30	0.900	14.69	6.32	<b>8.0</b>	<b>0.1</b>		

\* α-ejection correction (Farley et al., 1996) calculated using mass-weighted mean radii.  
† Effective uranium content, [eU] = [U] + 0.235 × [Th].  
§ Rejected by the weighted-mean age calculation using Isoplot (Ludwig, 2012).

TABLE S5. APATITE AND ZIRCON FISSION-TRACK DATA FROM THE JIACHA GORGE (U-CONTENT DETERMINED USING EXTERNAL-DETECTOR METHOD).

	Sample No.	Elev. (m)	n (age)	$\rho_s$ ( $10^4 \text{ cm}^{-2}$ )	$N_s$	$\rho_i$ ( $10^6 \text{ cm}^{-2}$ )	$N_i$	$\rho_d$ ( $10^5 \text{ cm}^{-2}$ )	$N_d$	$P(\chi^2)$ (%)	Age Dispersion (%)	Pooled Age $\pm 1\sigma$ (Ma)	U $\pm 2\sigma$ (ppm)	MTL $\pm 1SD$ ( $\mu\text{m}$ )	n (length)
AFT	14T20	4191	20	9.73	62	1.05	668	10.7	3417	97.6	0.2	<b>12.3 <math>\pm</math> 1.6</b>	15 $\pm$ 1	<b>13.13 <math>\pm</math> 1.52</b>	46
	14T21	4058	20	11.0	55	1.16	580	10.7	3428	87.2	0.5	<b>12.6 <math>\pm</math> 1.7</b>	16 $\pm$ 1		
	14T22	3912	40	8.04	70	1.05	917	10.8	3439	98.3	0.4	<b>10.2 <math>\pm</math> 1.2</b>	15 $\pm$ 1	<b>12.45 <math>\pm</math> 1.74</b>	<b>6</b>
	14T24	3660	20	9.74	72	1.40 $\times$	1035	10.8	3450	99.8	0.1	<b>9.3 <math>\pm</math> 1.1</b>	19 $\pm$ 1	<b>13.47 <math>\pm</math> 1.63</b>	42
	14T18	3477	26	7.67	76	1.21 $\times$	1197	10.7	3405	91.3	0.2	<b>8.4 <math>\pm</math> 1.0</b>	17 $\pm$ 1	<b>13.07 <math>\pm</math> 1.54</b>	46
	14T26	3376	20	13.3	108	2.92	2367	10.8	3461	93.5	0.4	<b>6.1 <math>\pm</math> 0.6</b>	40 $\pm$ 2	<b>13.89 <math>\pm</math> 2.42</b>	19
ZFT	14T20	4191	20	269	686	2.01	511	2.54	3162	63.4	0.1	<b>21.4 <math>\pm</math> 1.3</b>	119 $\pm$ 11		
	14T21	4058	20	294	698	2.16	513	2.54	3163	99.3	0.1	<b>21.6 <math>\pm</math> 1.3</b>	128 $\pm$ 12		
	14T22	3912	19	204	794	1.83	713	2.54	3163	33.9	4.7	<b>19.2 <math>\pm</math> 1.0</b>	108 $\pm$ 9		
	14T24	3660	20	443	1392	3.58	1125	2.54	3163	57.7	0.3	<b>19.7 <math>\pm</math> 0.9</b>	211 $\pm$ 14		
	14T18	3477	20	531	1529	3.38	974	2.54	3162	14.8	2.3	<b>25.0 <math>\pm</math> 1.1</b>	200 $\pm$ 14		
	14T26	3376	20	495	924	3.75	700	2.54	3163	100.0	0.1	<b>21.0 <math>\pm</math> 1.1</b>	221 $\pm$ 18		

Note:  $\rho_s$  is the spontaneous track density ( $\text{cm}^{-2}$ );  $N_s$  is the number of spontaneous tracks;  $\rho_i$  is the induced track density ( $\text{cm}^{-2}$ );  $N_i$  is the number of induced tracks;  $\rho_d$  is the track density on fluence monitor ( $\text{cm}^{-2}$ );  $N_d$  is the tracks counted on fluence monitor; n is the number of counted grains for age and track length;  $P(\chi^2)$  is the Chi-squared probability; MTL, mean track length; Ages (Ma) are determined using the external-detector method with  $\zeta$ -calibration and calculated using the computer program and equations in Brandon (1992). AFT samples were counted with a zeta calibration factor  $\xi = 247.47 \pm 6.05$  for glass dosimeter IRMM540R, and ZFT samples were counted with a zeta calibration factor  $\xi = 125.66 \pm 1.86$  for glass dosimeter IRMM541. U  $\pm 2\sigma$  is the average uranium concentration (ppm).

TABLE S6. APATITE (U-TH)/HE DATA FROM THE JIACHA GORGE.

Sample	<sup>4</sup> He (ncc)	Mass (mg)	Mean $F_T^*$	U ppm	Th ppm	Sm ppm	Th/U	[eU] <sup>†</sup> ppm	Uncorrected Age (Ma)	Age (Ma)	Error (±1s)	Weight Mean age (Ma)	Error (±1s)
14T20_Ap1 <sup>§</sup>	0.145	0.01014	0.80	7.80	3.8	117.6	0.49	8.7	13.3	<b>16.7</b>	<b>1.0</b>	<b>5.6</b>	<b>2.0</b>
14T20_Ap2	0.120	0.00685	0.77	27.50	25.1	246.2	0.91	33.4	4.3	<b>5.5</b>	<b>0.3</b>		
14T20_Ap3	0.020	0.00436	0.74	11.00	5.2	107.0	0.47	12.2	3.1	<b>4.1</b>	<b>0.3</b>		
14T20_Ap4	0.056	0.00410	0.77	18.60	5.1	213.1	0.28	19.8	5.6	<b>7.3</b>	<b>0.5</b>		
14T20_Ap5 <sup>§</sup>	0.081	0.00769	0.78	8.40	5.1	99.4	0.61	9.6	9.0	<b>11.4</b>	<b>0.7</b>		
14T24_Ap1	0.089	0.00949	0.80	19.30	11.9	98.1	0.62	22.1	3.5	<b>4.4</b>	<b>0.3</b>	<b>4.8</b>	<b>0.9</b>
14T24_Ap2	0.123	0.01443	0.82	11.20	7.0	153.7	0.62	12.8	5.4	<b>6.5</b>	<b>0.4</b>		
14T24_Ap3	0.065	0.00950	0.80	13.50	14.4	180.6	1.06	16.9	3.3	<b>4.1</b>	<b>0.3</b>		
14T24_Ap4	0.042	0.00857	0.76	9.30	15.2	94.5	1.64	12.9	3.1	<b>4.1</b>	<b>0.3</b>		
14T24_Ap5	0.096	0.01426	0.80	10.40	10.3	215.9	0.99	12.8	4.2	<b>5.2</b>	<b>0.3</b>		
14T26_Ap1	0.409	0.01995	0.85	31.60	4.4	174.0	0.14	32.6	5.1	<b>6.0</b>	<b>0.4</b>	<b>5.3</b>	<b>0.8</b>
14T26_Ap2	0.116	0.00360	0.75	70.60	11.7	288.7	0.17	73.3	3.6	<b>4.8</b>	<b>0.3</b>		
14T26_Ap3	0.129	0.01069	0.81	25.30	5.0	153.9	0.20	26.5	3.7	<b>4.6</b>	<b>0.3</b>		
14T26_Ap4	0.237	0.01238	0.82	30.80	5.5	199.7	0.18	32.1	4.9	<b>5.9</b>	<b>0.4</b>		
<sup>b</sup> 14T26_Ap5	0.979	0.00876	0.80	28.40	7.4	192.2	0.26	30.1	30.2	<b>37.9</b>	<b>2.4</b>		

\*  $\alpha$ -ejection correction (Farley et al., 1996) calculated using mass-weighted mean radii.  
† Effective uranium content, [eU] = [U] + 0.235 × [Th].  
§ Rejected by the weighted mean age calculation using Isoplot (Ludwig, 2012).

TABLE S7. ZIRCON (U-TH)/HE DATA FROM THE JIACHA GORGE.

Sample	<sup>4</sup> He (ncc)	Mass	Mean $F_T^*$	U (ppm)	Th (ppm)	Th/U	[eU] <sup>†</sup> ppm	Uncorrected Age (Ma)	Age (Ma)	Error (±1s)	<sup>b</sup> Weight Mean age (Ma)	Error (±1s)
14T24_Zr1	1.689	0.0035	0.74	455.16	188.79	0.43	499.52	7.4	<b>10.0</b>	<b>0.2</b>	<b>10.3</b>	<b>0.7</b>
14T24_Zr3	1.431	0.0034	0.75	359.85	153.87	0.44	396.01	8.1	<b>10.8</b>	<b>0.3</b>		
14T24_Zr4	2.050	0.0030	0.75	693.11	214.26	0.32	743.46	7.0	<b>9.4</b>	<b>0.2</b>		
14T24_Zr5	2.202	0.0041	0.76	445.67	188.03	0.43	489.85	8.4	<b>11.1</b>	<b>0.2</b>		
14T26_Zr1	1.578	0.0025	0.73	558.46	230.15	0.42	612.54	7.7	<b>10.5</b>	<b>0.2</b>	<b>9.8</b>	<b>0.6</b>
14T26_Zr2	3.929	0.0041	0.78	917.88	272.39	0.30	981.89	7.5	<b>9.6</b>	<b>0.2</b>		
14T26_Zr3	0.802	0.0016	0.68	548.76	284.78	0.53	615.69	6.2	<b>9.1</b>	<b>0.2</b>		

\*  $\alpha$ -ejection correction (Farley et al., 1996) calculated using mass-weighted mean radii.  
† Effective uranium content, [eU] = [U] + 0.235 × [Th].